NJC

Theoretical study of CO_2 adsorption on Pt

Journal:	*New Journal of Chemistry*
Manuscript ID	NJ-LET-06-2019-003092.R1
Article Type:	Letter
Date Submitted by the Author:	17-Jul-2019
Complete List of Authors:	Matsuda, Shofu; Nagaoka University of Technology, Department of Materials Science and Technology Mukai, Tsuyoshi; Nagaoka University of Technology Sakurada, Seishiro; Nagaoka University of Technology Uchida, Nozomu; Nagaoka University of Technology Umeda, Minoru; Nagaoka University of Technology, Materials Science and Technology, Faculty of Engineering

NJC

LETTER

Theoretical study of CO_2 adsorption on Pt

Shofu Matsuda,[a] Tsuyoshi Mukai,[a] Seishiro Sakurada,[a] Nozomu Uchida,*[a] and Minoru Umeda *[a]

Received 00th January 20xx,
Accepted 00th January 20xx

DOI: 10.1039/x0xx00000x

www.rsc.org/

The process of CO_2 adsorption on a Pt electrocatalyst was investigated computationally. We found that CO_2 adsorption on Pt crystals proceeds spontaneously in the presence of H_2O and H both adsorbed on Pt, attributed to hydrogen bond formation and charge rearrangement interactions.

Introduction

CO_2 chemical fixation is a valuable method for energy storage and resource recovery, unlike carbon capture and storage (CCS)[1] and the physical immobilization of CO_2.[2] CO_2 electroreduction is attractive for practical applications because, theoretically, the reaction occurs at a potential close to that of H_2 generation by H_2O reduction.[3] However, practically, CO_2 electroreduction using Cu, Au, or Ag electrocatalysts requires a very large overpotential of ~1 V.[4–11] Thus, it is challenging to reduce CO_2 with less energy than that required for H_2 production by H_2O electrolysis. On the other hand, when using a Pt electrocatalyst, CO_2 can be reduced with a low overpotential (0–0.3 V vs. reversible hydrogen electrode (RHE))[12,13] and CO is left adsorbed on the electrode surface.[14,15] The theoretical CO_2/CO redox reaction is as follows.[16]

$$CO_2 + 2H^+ + 2e^- = CO + H_2O \ (E° = -0.106 \text{ V vs. standard hydrogen electrode (SHE)}) \quad (1)$$

Compared to the theoretical potential, the experimentally observed CO_2 reduction potential is more positive, which contributes to the strong adsorption of CO to Pt.[17,18] This strong adsorption has also been shown by theoretical calculations.[19]

However, it is difficult to obtain products by the further reduction of the CO_2-reduction intermediate adsorbed on the Pt electrode (CO_{ads}). Jaramillo et al. reported the production of small amounts of CH_4 and CH_3OH as products of CO_2 reduction on a Pt electrocatalyst at –1.5 V vs. RHE.[20] In contrast, in our previous study, CH_3OH was obtained by CO_2 electroreduction at 0.06–0.25 V vs. RHE using a membrane electrode assembly containing a Pt/C electrocatalyst, although the coulombic efficiency was still low.[21,] Remarkably, this result indicates that the production of useful materials by CO_2 reduction using a Pt electrocatalyst can occur with an extremely low overpotential.

Therefore, the detailed study of the CO_2 reduction process on the Pt electrocatalyst is particularly important. In particular, the investigation of each reduction reaction step is crucial. Herein, we focus our attention on the step in which CO_2 is reduced to Pt-CO_{ads}. In this step, CO_2 adsorption on the Pt electrocatalyst is assumed to occur as a pre-reaction; then, the adsorbed CO_2 should become the CO_{ads}. However, to date, the CO_2 adsorption process on Pt has not been clarified although there are some reports.[22-26] For example, CO_2 reduction process is successfully explained as proton-coupled electron transfer steps for Cu catalyst,[27] but not for Pt catalyst.[25] In this study, the investigation of CO_2 adsorption on Pt crystals in the presence of H_2O was conducted using computational chemistry methods.

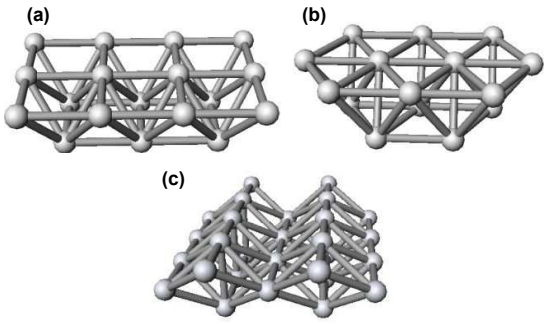

Fig. 1 Computationally calculated Pt clusters: (a) $Pt_{18}(100)$, (b) $Pt_{15}(111)$, and (c) $Pt_{28}(110)$.

[a] *Department of Materials Science and Technology, Graduate School of Engineering, Nagaoka University of Technology, 1603-1 Kamitomioka, Nagaoka, Niigata 940-2188, Japan*
E-mail: mumeda@vos.nagaokaut.ac.jp, solgel2@vos.nagaokaut.ac.jp

† Electronic Supplementary Information (ESI) available: [details of any supplementary information available should be included here]. See DOI: 10.1039/x0xx00000x

Results and discussion

Analysis of CO_2 adsorption on Pt crystal clusters

Fig. 1 shows the calculated Pt clusters. First, we performed structural optimization and vibrational calculations after placing a CO_2 molecule near the Pt clusters. In the optimizations of the Pt (100) and (111) faces, which have a high surface atomic density (1.3×10^{15} cm^{-2} for Pt (110) and 1.5×10^{15} cm^{-2} for Pt (111)), as shown in Figs. 1a and 1b, respectively, CO_2 adsorption was not observed. This could be because the interaction between CO_2 and Pt is quite weak. In contrast, a structure with adsorbed CO_2 was obtained for the Pt (110) cluster (Fig. 1c) whose surface atomic density was calculated to be 9.2×10^{14} cm^{-2}. This trend agrees well with experimental data for CO_2-reduction activity of each face.[28,29] However, the value of ΔG_{ads}, which is defined in the Computational details, was calculated to be +49.2 kJ/mol for Fig. 1c, indicating that the adsorption of CO_2 alone on a Pt catalyst is difficult. Because a crystal-face dependence of CO_2 adsorption was observed, we employed the Pt (110) cluster (Fig. 1c) in the subsequent calculations.

Fig. 2 shows the effect of adsorbed H_2O molecules (H_2O_{ads}) on CO_2 adsorption to the Pt (110) cluster. The calculations were performed using 0, 1, 2, 3, and 4 H_2O molecules. It should be noted that ΔG_{ads} becomes negative on the introduction of H_2O_{ads}. Furthermore, as the number of H_2O_{ads} increases, ΔG_{ads} becomes more negative. In the case of 4 H_2O_{ads}, ΔG_{ads} was calculated to be -147 kJ/mol. However, ΔG for the H_2O-adsorbed state without CO_2 adsorption is more negative than the value ΔG_{ads} shown in Fig. 2. For example, the value of ΔG for four adsorbed H_2O molecules without CO_2 adsorption was calculated to be around -180 kJ/mol. Furthermore, the results indicate that CO_2 does not adsorb to Pt having three or four adsorbed H_2O molecules, possibly because of the steric hindrance. Therefore, CO_2 adsorption to the Pt surface does not occur spontaneously. Considering the differences from the previous experimental research,[12-14] we suggest that H^+ adsorption affects the adsorption of CO_2 on Pt.

Effect of H_3O^+ on CO_2 adsorption

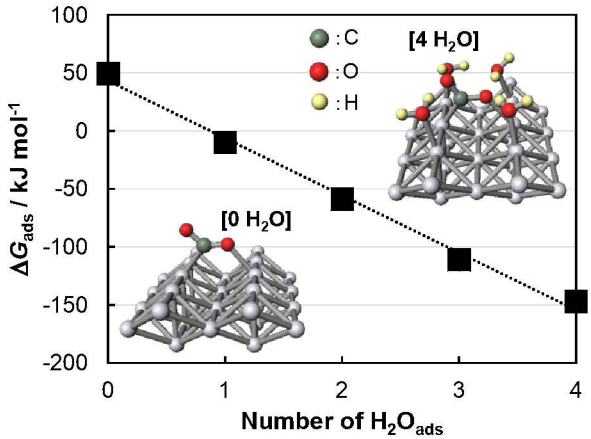

Fig. 2 Influence of the number of adsorbed H_2O molecules on ΔG_{ads} for CO_2 adsorption at Pt (110). Inserted models show the CO_2-adsorbed states with 0 and 4 H_2O_{ads}.

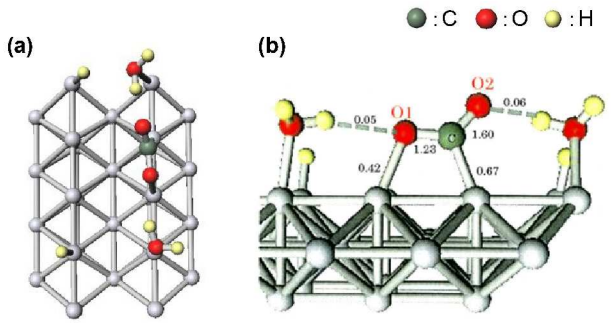

Fig. 3 (a) The most stable CO_2-adsorbed state and (b) bond orders.

Assuming that two molecules of H_3O^+ are adsorbed on the Pt (110) surface, we next performed structural optimization and vibrational calculations with six adsorption patterns in consideration of cluster symmetry. As a result, (see Fig. S1 in the Electronic Supplementary Information (ESI)†), we found that two molecules of H_3O^+ were separated into two H atoms and two H_2O molecules adsorbed on Pt (110). The values of ΔG for all six adsorption structures were negative (around -160 kJ/mol), which indicates that the adsorption of H_3O^+ onto Pt (the formation of H_{ads} and H_2O_{ads}) occurs spontaneously.

Subsequently, the structural optimization of nine adsorption patterns was conducted after placing a CO_2 molecule on the empty site of the H_3O^+-adsorbed Pt surface. In consequence, six cross-linked adsorption patterns of CO_2, such as that shown in Fig. 3a (the other five patterns are shown in Fig. S2 and Table S1 in the ESI†), whose ΔG_{ads} were calculated to be around -160 kJ/mol, were obtained. Three patterns for non-adsorbed CO_2 were also obtained, as shown in Fig. S3 in the ESI†. Significantly, there is almost no difference in the ΔG values of the CO_2-adsorbed state (Figs. 3a and S2) and ΔG for the CO_2 non-adsorbed state (Fig. S3). When the Boltzmann distribution was analyzed using the ΔG values obtained from the vibrational calculations, the abundance ratios of all nine adsorption patterns were found to be almost the same. Therefore, CO_2 adsorption on the Pt surface proceeds spontaneously. In the CO_2-adsorbed states, systems where CO_2 is adsorbed next to H_2O_{ads} are stable.

Fig. 3b shows the results of the calculation of the bond order in the CO_2-adsorbed state depicted in Fig. 3a. One reason why the CO_2 adsorption to Pt occurs spontaneously could be the hydrogen bonds occurring between the oxygen atom of CO_2 and the hydrogen atom of H_2O, as shown in Fig. 3b. These hydrogen bonds stabilize the CO_2 adsorbed on Pt. Remarkably, Fig. 3b also reveals that the bond orders for both of C=O1 (1.23) and C=O2 (1.60) are less than 2. In other words, adsorption on Pt increases the bond length of the C=O bonds of the adsorbed CO_2, which could induce a cleavage (yielding CO_{ads}). Based on the experimental analysis,[14,15] CO_2 is reduced to Pt-CO_{ads}. However, the C=O bond orders are much higher than the bond orders of O-Pt (0.42), as shown in Fig. 3b. Hence, it is suggested that the cleavage of C=O bond does not occur without the participation of further e^- or H^+. Although the mechanism of transformation of adsorbed CO_2 to CO_{ads} on the Pt surface is not known in detail,

further investigation, such as the study of H_{ads} migration, should yield significant clues concerning the subsequent reaction processes.

Table 1 Mulliken charges of each molecule for CO_2 non-adsorbed state (Fig. S3a) and CO_2-adsorbed state (Fig. 3a).

	Mulliken charge	
	Non-adsorbed CO_2	Adsorbed CO_2
Pt	-0.690	-0.234
H	-0.022	-0.051
H	-0.022	-0.052
H_2O	0.271	0.239
H_2O	0.280	0.290
CO_2	0.095	-0.398

Mulliken population analysis

To understand the state of the bonds in the system with CO_2 adsorbed on Pt in detail, Mulliken population analysis[30] was conducted for both adsorbed and non-adsorbed CO_2 (Figs. 3a and S3a) states. The results are listed in Table 1. The charges of the two H_2O_{ads} are partially positive, and the charges of Pt and two H_{ads} are partially negative in both states; thus, charge rearrangement between H_2O_{ads}, Pt, and H_{ads} is confirmed. It should be noted that the Mulliken charge of CO_2 is partially negative for the adsorbed CO_2, whereas it is partially positive for non-adsorbed CO_2. Therefore, charge rearrangement occurs not only for H_2O_{ads}, Pt, and H_{ads} but also for adsorbed CO_2 in the CO_2 adsorption process, which is indicative of electron donor–electron acceptor interactions between the adsorbed CO_2, Pt, H_{ads}, and H_2O_{ads} in the CO_2 adsorption process. Consequently, this charge rearrangement interaction stabilizes the CO_2 adsorbed on Pt.

Computational details

All calculations in this study were conducted with Becke's three-parameter hybrid exchange functional with Lee–Yang–Parr correlation functional (B3LYP) as implemented in Gaussian 09. The LANL2DZ[31] basis set was used for Pt, whereas the 6-31G**[32] basis set was used for H, C, and O. The charge of H_3O^+ molecules was specified in the input file as the charge of the whole system. Molecular models were created using the Winmostar™ (X-Ability Co., Ltd., Tokyo, Japan). We performed structural optimization and vibrational calculations for all models to calculate the Gibbs free energy of adsorption (ΔG_{ads}), which is defined by the following equations.

$$\Delta G_{ads} = \Delta G \text{ (after adsorption)} - \Delta G \text{ (before adsorption)} \quad (2)$$

$$\Delta G \text{ (before adsorption)} = \Delta G \text{ (adsorbed)} + \Delta G \text{ (Pt cluster)} \quad (3)$$

$$\Delta G = \Delta H - T\Delta S \quad (4)$$

Here, ΔH is the enthalpy, T is the temperature (298.15 K), and ΔS is the entropy. ΔS was estimated considering the molecular vibration with the translation and rotation of the system. In the case of the calculation of the interatomic bond order, we used Natural Bond Orbital (NBO) analysis.[33] Note that we employed a two-layer Pt (110) cluster to obtain energies close to those of the experimental system. The calculation for the two-layer type of Pt (110) cluster was performed using the HA800tc/HT210 supercomputer (Research Institute for Information Technology, Kyushu University, Japan).

Conclusions

With the objective of identifying the CO_2 adsorption process on Pt crystals, we performed structural optimization and vibration calculations for each Pt model in the presence of CO_2, H_2O, and H_3O^+. The following conclusions are drawn.

(1) The adsorption of CO_2 alone on Pt does not occur.

(2) Although ΔG for CO_2 adsorption (ΔG_{ads}) is positive without H_2O_{ads}, ΔG_{ads} becomes negative on the introduction of H_2O_{ads} onto the Pt (110) cluster.

(3) The adsorption of H_3O^+ onto Pt, which forms Pt-H and Pt-H_2O, occurs spontaneously.

(4) CO_2 adsorption on Pt crystals is spontaneous in the presence of Pt-H_2O and Pt-H.

(5) A hydrogen bond is formed between H_2O and CO_2 both adsorbed on Pt.

(6) Charge rearrangement interactions between adsorbed CO_2, Pt, H_{ads}, and H_2O_{ads} occur in the CO_2 adsorption process.

These findings will assist in the strategic design of electrochemical processes for the conversion of CO_2 into useful compounds using Pt electrocatalysts, although further investigation, such as the elucidation of the mechanism of the reaction process from the adsorbed CO_2 to CO_{ads}, is necessary.

Conflicts of interest

There are no conflicts to declare.

Acknowledgement

This work was supported by the Japan Science and Technology Agency (JST) through the Advanced Catalytic Transformation Program for Carbon Utilization (ACT-C, Grant Number JPMJCR12Y4).

Notes and references

1 M. Bui, C. S. Adjiman, A. Bardow, E. J. Anthony, A. Boston, S. Brown, P. S. Fennell, S. Fuss, A. Galindo, L. A. Hackett, J. P. Hallett, H. J. Herzog, G. Jackson, J. Kemper, S. Krevor, G. C. Maitland, M. Matuszewski, I. S. Metcalfe, C. Petit, G. Puxty, J. Reimer, D. M. Reiner, E. S. Rubin, S. A. Scott, N. Shah, B. Smit, J. P. M. Trusler, P. Webley, J. Wilcox and N. M. Dowell, *Energy Environ. Sci.*, 2018, **11**, 1062.
2 M. P.-Titus, *Chem. Rev.*, 2014, **114**, 1413.
3 Y. Zhang, M. Xie, V. Adamaki, H. Khanbareh and C. R. Bowen, *Chem. Soc. Rev.*, 2017, **46**, 7757.
4 Y. Hori, K. Kikuchi and S. Suzuki, *Chem. Lett.*, 1985, **14**, 1695.
5 C. S. Chen, A. D. Handoko, J. H. Wan, L. Ma, D. Ren and B. S. Yeo, *Catal. Sci. Technol.*, 2015, **5**, 161.

6 R. Reske, H. Mistry, F. Behafarid, B. R. Cuenya and P. Strasser, *J. Am. Chem. Soc.*, 2014, **136**, 6978.
7 A. Loiudice, P. Lobaccaro, E. A. Kamali, T. Thao, B. H. Huang, J. W. Ager and R. Buonsanti, *Angew. Chem., Int. Ed.*, 2016, **55**, 5789.
8 W. L. Zhu, R. Michalsky, Ö. Metin, H. F. Lv, S. J. Guo, C. J. Wright, X. L. Sun, A. A. Peterson and S. H. Sun, *J. Am. Chem. Soc.*, 2013, **135**, 16833.
9 X. F. Feng, K. L. Jiang, S. S. Fan and M. W. Kanan, *J. Am. Chem. Soc.*, 2015, **137**, 4606.
10 C. Kim, H. S. Jeon, T. Y. Eom, M. S. Jee, H. J. Kim, C. M. Friend, B. K. Min and Y. J. Hwang, *J. Am. Chem. Soc.*, 2015, **137**, 13844.
11 Q. Lu, J. Rosen, Y. Zhou, G. S. Hutchings, Y. C. Kimmel, J. G. G. Chen and F. Jiao, *Nat. Commun.*, 2014, **5**, 149.
12 J. Giner, *Electrochim. Acta*, 1963, **8**, 857.
13 Y. Niitsuma, K. Sato, S. Matsuda, S. Shironita and M. Umeda, *J. Electrochem. Soc.*, 2019, **166**, F208.
14 M. W. Breiter, *Electrochim. Acta*, 1967, **12**, 1213.
15 B. Beden, A. Bewick, M. Razaq and J. Weber, *J. Electroanal. Chem.*, 1982, **139**, 203.
16 A. J. Bard, R. Parsons and J. Jardan, *Standard Potentials in Aqueous Solution*, Marcel Dekker, Inc., New York and Basel, 1985.
17 S. Taguchi, A. Aramata and M. Enyo, *J. Electroanal. Chem.*, 1994, **372**, 161.
18 H. Furukawa, S. Matsuda, S. Tanaka, S. Shironita and M. Umeda, *Appl. Surf. Sci.*, 2018, **434**, 681.
19 M. T. M. Koper and R. A. van Santen, *J. Electroanal. Chem.*, 1999, **476**, 64.
20 K. P. Kuhl, T. Hatsukade, E. R. Cave, D. N. Abram, J. Kibsgaard and T. F. Jaramillo, *J. Am. Chem. Soc.*, 2014, **136**, 14107.
21 S. Shironita, K. Karasuda, K. Sato and M. Umeda, *J. Power Sources*, 2013, **228**, 68.
22 S. B. Brummer and K. Cahill, *J. Electroanal. Chem.*, 1969, **21**, 463.
23 J. M. Ricart, M. P. Habas, A. Clotet, D. Curulla and F. Illas, *Surf. Sci.*, 2000, **460**, 170.
24 C. Shi, C. P. O'Grady, A. A. Peterson, H. A. Hansen and J. K. Norskov, *Phys. Chem. Chem. Phys.*, 2013, **15**, 7114.
25 J. Hussain, H. Jonsson and E. Skulason, *Faraday Discussions*, 2016, **195**, 619.
26 X. Liu, L. Sun and W.-Q. Deng, *J. Phys. Chem. C*, 2018, **122**, 8306.
27 A. A. Peterson, F. Abild-Pedersen, F. Studt, J. Rossmeisl and J. K. Norskov, *Energy Environ. Sci.*, 2010, **3**, 1311.
28 N. Hoshi, T. Mizumura and Y. Hori, *Electrochim. Acta*, 1995, **40**, 883.
29 S. Taguchi and A. Aramata, *Electrochim. Acta*, 1994, **39**, 2533.
30 R. S. Mulliken, *J. Chem. Phys.*, 1952, **23**, 1833.
31 T. R. Cundari and W. J. Stevens, *J. Chem. Phys.*, 1993, **98**, 5555.
32 R. Ditchfield, W. J. Hehre and J. A. Pople, *J. Chem. Phys.*, 1971, **54**, 724.
33 J. E. Carpenter and F. Weinhold, *J. Mol. Struct.: Theochem*, 1988, **169**, 41.

Table of Contents Entry

Computational chemistry reveals that CO_2 is spontaneously adsorbed on a Pt (110) crystal in the presence of H_2O_{ads} and H_{ads}.

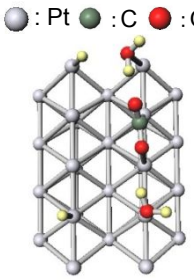

	Mulliken charge
Pt	-0.234
H	-0.051
H	-0.052
H_2O	0.239
H_2O	0.290
CO_2	-0.398